IEEE Photonics Journal
An IEEE Photonics Society Publication

Chromatic Dispersion Monitoring for NRZ-DPSK System Using Asynchronous Amplitude Histogram Evaluation

Volume 4, Number 4, August 2012

Zhao Wu
Yu Yu
Xinliang Zhang

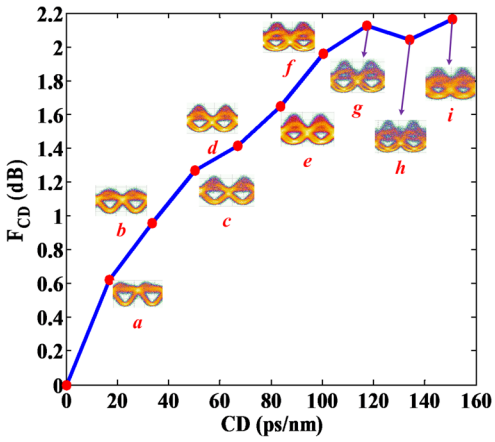

DOI: 10.1109/JPHOT.2012.2207451
1943-0655/$31.00 ©2012 IEEE

IEEE photonics SOCIETY
IEEE

Chromatic Dispersion Monitoring for NRZ-DPSK System Using Asynchronous Amplitude Histogram Evaluation

Zhao Wu, Yu Yu, and Xinliang Zhang

Wuhan National Laboratory for Optoelectronics, College of Optoelectronic Science and Engineering, Huazhong University of Science and Technology, Wuhan 430074, China

DOI: 10.1109/JPHOT.2012.2207451
1943-0655/$31.00 ©2012 IEEE

Manuscript received May 31, 2012; revised June 21, 2012; accepted June 29, 2012. Date of current version July 16, 2012. This work was supported in part by the National Basic Research Program of China under Grant 2011CB301704, by the Natural Science Fund for Distinguished Young Scholars under Grant 61125501, and by the National Natural Science Foundation of China under Grant 61007042. Corresponding author: X. Zhang (e-mail: xlzhang@mail.hust.edu.cn).

Abstract: We propose and demonstrate a chromatic dispersion (CD) monitoring technique for a nonreturn-to-zero differential phase-shift keying (NRZ-DPSK) signal generated with a Mach–Zehnder modulator at 40 Gb/s by analyzing the waveform overshoot after transmission. Without demodulating the NRZ-DPSK signal, the CD up to 120 ps/nm is monitored experimentally via the amplitude of the overshoot. Furthermore, based on the asynchronous amplitude histogram (AAH) evaluation method, a novel histogram processing method, which is more convenient, is proposed and investigated. Experimental results show that the monitoring scheme for CD is independent of optical signal-to-noise ratio (OSNR) within a certain range. This technique needs neither demodulating the signal nor extracting the synchronous clock, and it can be applied to high-order modulation formats at different bit rates.

Index Terms: Nonreturn-to-zero differential phase-shift keying (NRZ-DPSK), asynchronous amplitude histogram, optical performance monitoring, chromatic dispersion.

1. Introduction

Accurate chromatic dispersion (CD) monitoring is essential for optical communication system in order to achieve adaptive and exact dispersion compensation [1]. Various optical CD monitoring techniques have been proposed, such as 1) using asynchronous delay-tap sampling and extracting the parameters from the scattering plot [2]–[4]; 2) measuring the average variance of the received optical power [5]; 3) analyzing the radio-frequency (RF) power spectrum or clock tone after received with a photo-detector [6]–[8]; 4) utilizing the cross-phase modulation effect between the input signal and the inserted continuous-wave probe and investigating the output probe channel [9], [10]; and 5) inserting in-band subcarriers in the transmitter and monitoring their RF tones [11]. The asynchronous amplitude histogram (AAH) evaluation is a promising method for low-cost performance monitoring; it is easy to implement and does not need clock recovery [12]. Several AAH evaluation approaches have been reported for CD monitoring, such as 1) exploiting chirp-induced phase-to-amplitude modulation for the nonreturn-to-zero differential phase-shift keying (NRZ-DPSK) signal generated by the phase modulator [12]; 2) tracking the intensities at the valley of the waveform before demodulation for the return-to-zero DPSK (RZ-DPSK) signal [13], [14]; and 3) using an artificial neural network trained with AAH [15]. In practical optical communication system, the phase-modulated signals are mainly generated by a Mach–Zehnder modulator (MZM) for the low

chirping characteristic. In this paper, we use the AAH method to monitor CD via the amplitude of the overshoot after transmission for an MZM-modulated NRZ-DPSK signal.

On the other hand, many AAH evaluation approaches followed the method suggested by Carl *et al.* [16], mirroring the outer slope of the histogram of the marks to get a bell-shaped curve, from which Gaussian fitting can be done [17]–[19]. However, there still exists a difficult point on how to determine the appropriate symmetry axis to mirror the outer slope of the histogram to get a bell-shaped curve, since the curve is not always symmetry according to its peak in the AAH.

In this paper, a simple method for CD monitoring by using the amplitude of the overshoot is proposed and demonstrated. We further propose a different histogram processing method, which extracts the required parameters directly from a part of the outer slope of the histogram without mirroring the outer slope. The impact of an optical signal-to-noise ratio (OSNR) on the monitoring results for the NRZ-DPSK signal is also investigated. This scheme can be easily operated without extracting synchronous clock. It has the potential to be applied to an NRZ phase-modulated signal at higher bit rates and other advanced modulation formats.

2. Principle and Operation

2.1. Operation Principle for Monitoring

Generally, the NRZ-DPSK signal is generated by an MZM, which always produces an exact "π" phase-jump at the expense of residual optical intensity dip located in a phase transition point [20]. Considering a fiber-optical transmission system with a DPSK signal, the envelope of the electric field is expressed as

$$E(t) = \sum_{k=-\infty}^{+\infty} a_k g(t - kT_s) \tag{1}$$

where $a_k \in \{-1, 1\}$ are information symbols that are independently and identically distributed, T_s is the symbol period, and $g(t)$ is the pulse shape

$$g(t) = \exp\left[-\frac{1}{2}\left(\frac{t}{T}\right)^{2m}\right]. \tag{2}$$

Generally, for an NRZ-DPSK signal, $m \geq 5$, and $g(t)$ is regarded as a super-Gaussian pulse or even a square pulse. Consecutive pulses with unchanged phase can be considered as a wide super-Gaussian pulse.

Neglecting the attenuation and nonlinear effect of fiber, it is known that a Gaussian-shaped pulse still remains Gaussian shape when deteriorated by the CD [21]. However, it is rather different for a super-Gaussian-shaped pulse after impaired by CD. The simulated results are presented in Fig. 1(a) using the commercial software Virtual Photonics Inc. (VPI). Super-Gaussian pulses before and after transmitting through a single-mode fiber (SMF) are illustrated in blue-solid and red-dash curves, respectively. The simulated results show that there exist overshoots at both the rising and trailing edges of the pulses, and it looks like ear of the pulse. With increasing of CD, the amplitude of the overshoot will increase accordingly [as indicated by the arrow i) in Fig. 1(a)]. On the other hand, the rising and trailing time of the pulse increases, and the upper part of the pulse becomes narrow [as indicated by the arrow ii) in Fig. 1(a)] while the lower part of the pulse is broadened by CD [as indicated by the arrow iii) in Fig. 1(a)]. Meanwhile, tiny ripples appear along with the large overshoots.

For the NRZ-DPSK signal impaired by CD, the pulses $g(t)$ are broadened. This induces destructive interference at the boundary between the two bits with opposite phases, as shown in Fig. 1(b). As a result, the intensity of the dips remains zero, and the overshoot increases with increasing of CD. However, the destructive interference at the boundary does not induce variation of the overshoot amplitude, which relates to the CD. Hence, the amplitude of the overshoot is used

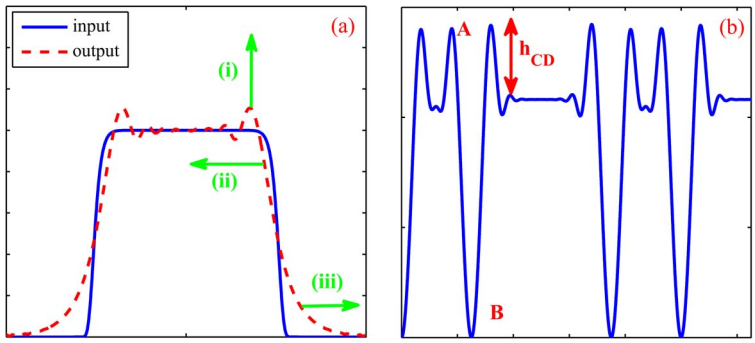

Fig. 1. (a) Super-Gaussian pulse impaired by CD. (b) Waveform of the NRZ-DPSK signal impaired by CD.

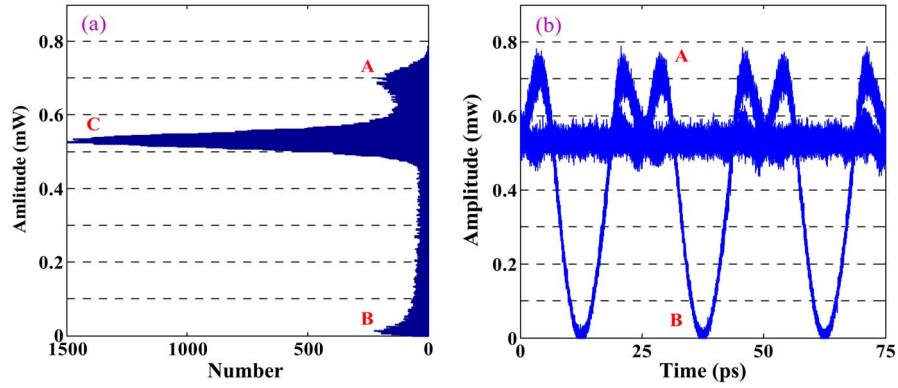

Fig. 2. (a) Histogram and (b) eye diagram of the NRZ-DPSK signal impaired by CD.

to monitor the CD of fiber. The overshoot and the dip in the NRZ-DPSK waveform are indicated by "A" and "B," respectively. The amplitude of the overshoot is defined as h_{CD}.

Then, the parameter F_{CD} is introduced, which is the function of the accumulated CD

$$F_{CD} = 10\log_{10}\left(\frac{h_{CD}}{P_0} + 1\right) \tag{3}$$

where P_0 is the amplitude of the original NRZ-DPSK signal, and h_{CD} is the amplitude of the overshoot.

The AAH evaluation method is used to measure h_{CD}. The histogram and the eye diagram of the NRZ-DPSK signal impaired by the CD are illustrated in Fig. 2(a) and (b), respectively. There are three peaks in the histogram, which represent three intensity levels of the NRZ-DPSK waveform, respectively. In Fig. 2(a), peak B is yielded due to the intensity dip in the NRZ-DPSK waveform. The position of peak B remains near zero because of the destructive interference between the neighboring bits with "π" phase difference. Peak C is corresponding to the amplitude of the signal [i.e., P_0 in (3)]. The variance of peak C is the result of the amplified spontaneous emitted (ASE) noise and the tiny ripple in the waveform induced by the CD. Peak A presents the overshoot of the NRZ-DPSK signal. The location of peak A responds to the CD.

2.2. Mathematical Algorithm

Peak A in the AAH is used for curve fitting to measure the dispersion. As shown in Fig. 2(a), the three obvious peaks in the AAH are considered as the summation of three Gaussian-shaped curves. The following task is to determine the location of peak A. To solve this problem, many

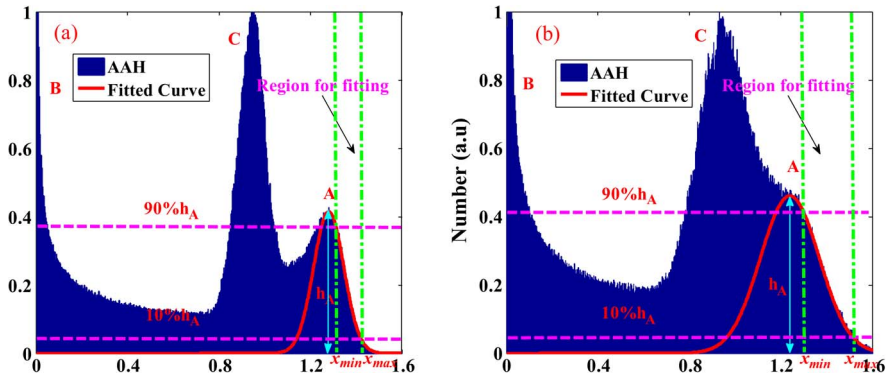

Fig. 3. Gaussian curve fitting for the AAH under (a) high and (b) low OSNR.

people follow the method suggested by Carl *et al.* [16], mirroring the outer slope of the histogram of the marks to get a bell-shaped curve, from which Gaussian fitting can be done. However, it is rather difficult to determine the proper symmetry axis, since the symmetry axis is not always located at peak A in the AAH. Furthermore, it is hard to identify the symmetry axis when the OSNR is low, since peak A is submerged by peak C [see Fig. 3(b)]. Here, a different method is proposed to get the parameters from the AAH. This method extends the tolerance of OSNR for curve fitting. In fact, each of the peaks in AAH is not a perfect Gaussian shape because of the superposition between the adjacent peaks, whereas the outside part of peak A in AAH is free from the overlap disturbing. Thus, the accurate parameter can be got from this part of the incomplete Gaussian distribution.

The envelope of the AAH is defined as parameter$y$, uninfluenced region is set as $[x_{\min}, x_{\max}]$. Then, a Gaussian-shaped function $f(x) = M\exp(-((x-\mu)^2/2\sigma^2))$ is configured, which is determined by three parameters $[M, \mu, \sigma]$.μ is considered as the location of peak A if $f(x)$ matches well with peak A in the AAH. In this scheme, only a part of incomplete Gaussian distribution in the AAH is needed to match peak A with $f(x)$ nicely. The final task of the work is to make $f(x)$ to match the AAH within the region $[x_{\min}, x_{\max}]$ as accurate as possible. In other words, the appropriate parameters $[M, \mu, \sigma]$ in 3-D space should be calculated out to get the minimum of norm $\|f-y\|$. $\|f-y\|$ is defined as

$$\|f-y\| = \sqrt{\sum_{i=1}^{N}[f(x_i)-y_i]^2} \tag{4}$$

where x_i is the sliced points from $x_{\min}$ to $x_{\max}$, and y_i is the point from AAH.

In this paper, the nonlinear conjugate gradient method with an iteration process is taken to get the optimal parameters. As illustrated in Fig. 3(a), the region $[x_{\min}, x_{\max}]$ is defined as the section between two vertical lines, which are shown in green-dash. In practical, a larger region achieves a faster iteration process to reach convergence. However, the larger region will comprise more noise. In this paper, $x_{\min}$ is at the 90% of the maximum of peak A [i.e., h_A in Fig. 3(a)], whereas $x_{\max}$ is at the 10% of h_A. The fitted curve is an ideal Gaussian shape, which is marked in red-solid. The fitted curve fits well with AAH plot in the region $[x_{\min}, x_{\max}]$. Hence, the parameters of peak A are obtained from the Gaussian-shaped curve.

However, it is unconceivable to determine the symmetry axis directly using the previous method, when the OSNR is too low and peak A is buried in peak C, as shown in Fig. 3(b). Fortunately, the inflection point A in the AAH can still be easily found. In this technique, the height of the inflection point can also be intended as h_A, which is similar to the maximum of peak A in Fig. 3(a). The region from 10% to 90% of h_A is used for Gaussian curve fitting. Before iteration, μ is initialized with an estimated value around the location of peak A (or the inflection point if peak A is buried in peak C).

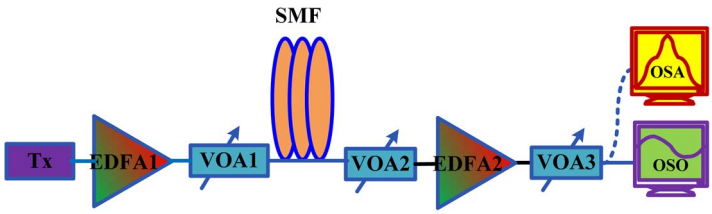

Fig. 4. Schematic setup for the proposed method.

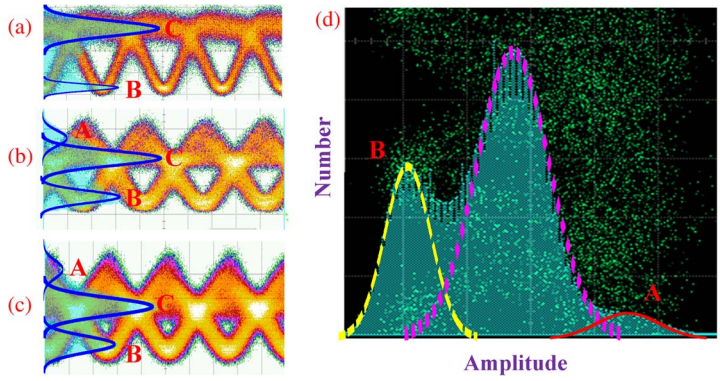

Fig. 5. Eye diagram and AAH of the (a) original signal; (b) signal transmitted through 3-km SMF; (c) signal transmitted through 5-km SMF; (d) AAH for Gaussian curve fitting.

An accurate μ value can be got after the iteration process. However, this method is not suitable yet when the OSNR is too low.

3. Experiment and Result

The proposed monitoring technique for 40-Gb/s NRZ-DPSK systems is shown in Fig. 4. A distributed feedback (DFB) laser operating at 1554.28 nm is externally modulated to a DPSK signal by a $LiNbO_3$ MZM, which is driven by a $2^{31} - 1$ pseudorandom binary sequence signal at 39.81 Gb/s. An erbium-doped fiber amplifier (EDFA1) and a variable optical attenuator (VOA1) are used to adjust the optical power to 0 dBm, ensuring the negligible nonlinear effects in the fiber. A preset CD is realized by using a standard SMF with premeasured length. At the end of the fiber, the OSNR of the optical signal is adjusted by tuning the following VOA2 before EDFA2. The optical power is adjusted to 0 dBm again by the next VOA3. The OSNR is measured by the Auristsu MS9710C optical spectrum analyzer (OSA) with 0.1-nm resolution. Finally, the optical signal without demodulation is directly detected and analyzed by an Agilent 86100C digital optical sampling oscilloscope (OSO), which contains an electric filter with bandwidth of 39.8 GHz to eliminate the redundant ASE noise. 1350 points are got out from the oscilloscope every time, and 10 times are repeated to construct the histogram.

The eye diagram and its corresponding AAH of the signal are illustrated in Fig. 5(a)–(c). Fig. 5(a) shows the eye diagram and AAH of the original NRZ-DPSK signal. There are two clear peaks in the AAH, which represent the amplitude and the intensity dip of the NRZ-DPSK signal, respectively. Fig. 5(b) and (c) shows the eye diagrams and AAHs of the signal transmitting through a span of 3- and 5-km SMF, respectively. Compared with Fig. 5(a)–(c) presents an overshoot in the eye diagram, and a peak appears accordingly in the AAH. The amplitude of the overshoot increases with the increase in the fiber length, and peak A in the AAH moves far away from peak C gradually. Fig. 5(d) shows the AAH for Gaussian curve fitting; the AAH is regarded as the combination of three Gaussian-shaped pulses presented as a yellow dash, a pink dot, and solid red, respectively.

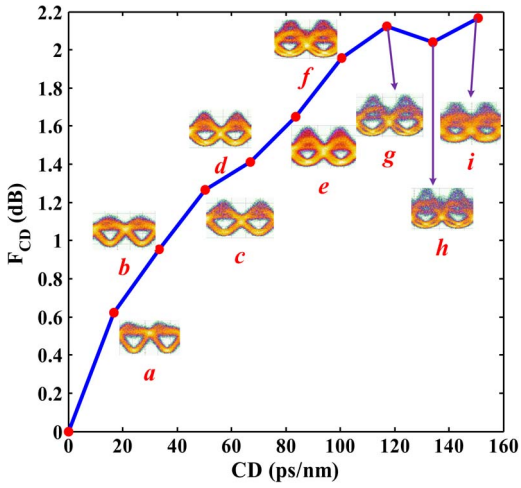

Fig. 6. Monitoring result of CD for 40-Gb/s NRZ-DPSK signal.

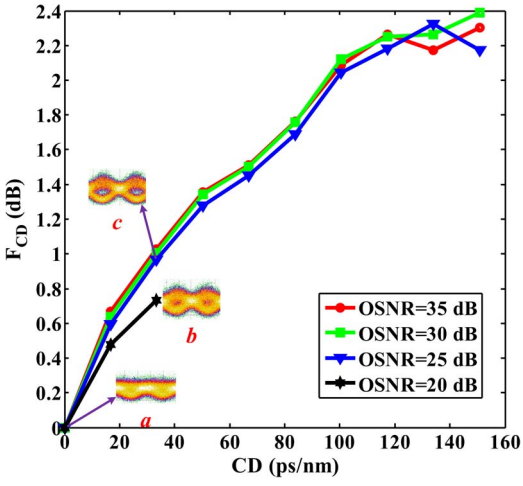

Fig. 7. F_{CD} versus different cumulated dispersion under different OSNRs.

Gaussian curve fitting for the AAH is performed with the method proposed in Section 2. Fig. 6 shows the results of F_{CD} under different CDs for NRZ-DPSK system when the OSNR is 35 dB. F_{CD} changes by around 2 dB when the CD varies from 0 to 120 ps/nm. When the CD increases to 120 ps/nm or more, the eye diagrams of the signals become closed with increasing of CD, and the AAH got from the asynchronous samplings become vague. This limits the monitoring range. The inserting pictures (a)–(i) show the eye diagrams of NRZ-DPSK signals with different CDs. The amplitude of the overshoot in the eye diagram increases with increasing of CD monotonically when CD increases from 0 to 120 ps/nm, and the eye opening decreases accordingly.

4. Discussion

The ASE noise induced by the transmission link broadens the peaks in the AAH, but it does not change the locations of the peaks. In this paper, only the locations of the peaks in AAH are used to get precise monitoring result from the signals. The impact of OSNR on CD monitoring results is also experimentally investigated.

The measured results for CD under different OSNRs of 20, 25, 30, and 35 dB are illustrated in Fig. 7. The technique works well for OSNR higher than 20 dB. The plots are closer when OSNRs

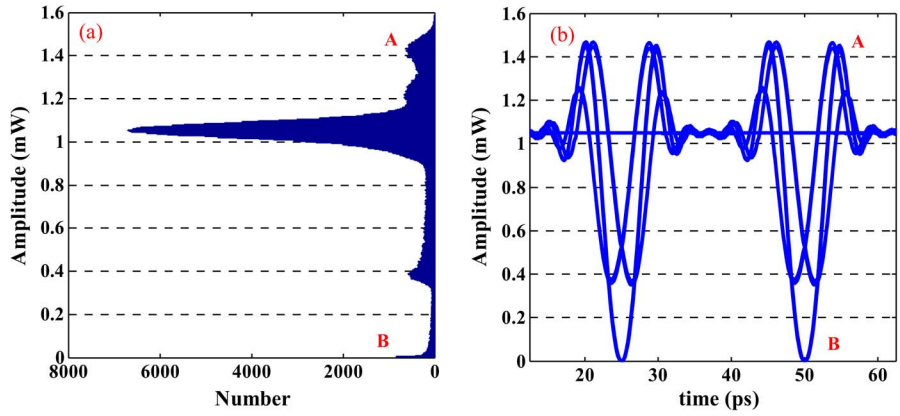

Fig. 8. (a) Histogram and (b) eye diagram of the NRZ-DQPSK signal impaired by CD.

are 30 and 35 dB, compared with the plot under OSNR of 25 dB. The curve fitted results are hardly credible when CD exceeds 120 ps/nm; they differ greatly under different OSNRs. The inserting pictures (a)–(c) show the eye diagrams of original signal under OSNR of 20 dB, CD-impaired signal under OSNRs of 20 and 25 dB, respectively. The eye diagram is nearly closed when OSNR is 20 dB; this induces large fitting error for CD monitoring. Comparing the inserting pictures (b) and (c), it can be seen that the ASE noise broadens the eyelid of the eye diagram. This limits the OSNR tolerance of this scheme.

The effects of PMD and phase noise affect the performance of the method. The PMD-induced overlap cannot result in destructive or constructive interference between the two orthogonal polarizations. As the overshoot in the NRZ-DPSK signal has been raised by the CD, the additional PMD reduces the amplitude of the overshoot due to the misalignment between two orthogonal polarizations. As a result, the amplitude of the overshoot increases with increasing of CD while it decreases with an increase of differential group delay (DGD). However, the influence of PMD can be eliminated when the polarization state of the incoming signal is aligned with one of the two principal states of polarization (PSPs) of the fiber.

The phase noise of the signal is converted into intensity noise after propagating through a section of dispersion fiber, and the intensity noise induces the degradation of the OSNR. Whereas, in this manuscript, the data processing method extends the OSNR tolerance compared with the previous method. Thus, the phase noise has little effect on the monitoring results.

The electric filter contained in the OSO is used to eliminate the redundant ASE noise. However, it changes the monitoring results simultaneously, since the electric filter changes the waveform of the signal. More specifically, a narrow-band filter increases the rising and trailing time of the pulse. As a result, the amplitude of the overshoot changes more slowly with CD. This extends the tolerance of CD and increases the monitoring range. As a result, a larger monitoring range is achieved in the existence of a narrow-bandwidth filter, at the expense of lower monitoring sensitivity. The monitoring results are still fixed when the effect of the filter in the system is considered.

The proposed scheme is also suitable for differential quadrature phase-shift keying (DQPSK) format generated by nested MZMs. From the point of view of a linear system, the electric field of the NRZ-DQPSK signal is recognized as a combination of two coherent NRZ-DPSK signals, which carry independent data. The eye diagram and corresponding AAH of the CD-impaired NRZ-DQPSK signal are illustrated in Fig. 8(a) and (b), respectively. There are two heights of overshoots and two depths of dips in the NRZ-DQPSK signal. Five peaks in the AAH are corresponding to five intensity levels in the NRZ-DQPSK waveform. The larger overshoot [point A in Fig. 8(b)] can be used to monitor the CD for NRZ-DQPSK system similar to NRZ-DPSK system.

The monitoring range is different for these NRZ phase-modulated signals, since the CD is monitored based on the AAH evaluation method. The impact of CD rises precipitously as the square of the symbol rate, and the monitoring range is reduced accordingly.

5. Conclusion

In this paper, a simple CD monitoring technique for NRZ-DPSK system has been proposed and demonstrated based on the AAH evaluation method. The CD is measured within a range of 0–120 ps/nm experimentally by measuring the amplitude of the overshoot of the NRZ-DPSK signal. The impact of OSNR on the CD monitoring result is also investigated. In the part of the AAH evaluation, the AAH is fitted with a nonlinear conjugate gradient method by constructing the optimal function at an appropriate region, making the treatment more convenient and reliable. The scheme can be applied to different bit rates, and it has the potential to be easily applied to MZM-generated high-order NRZ phase-modulated signals.

References

[1] C. C. K. Chan, *Optical Performance Monitoring: Advanced Techniques for Next-Generation Photonic Networks*. Amsterdam, The Netherlands: Elsevier, 2010.

[2] J. Zhao, Z. Li, D. Liu, L. Cheng, C. Lu, and H. Y. Tam, "NRZ-DPSK and RZ-DPSK signals signed chromatic dispersion monitoring using asynchronous delay-tap sampling," *J. Lightw. Technol.*, vol. 27, no. 23, pp. 5295–5301, Dec. 1, 2009.

[3] T. B. Anderson, A. Kowalczyk, K. Clarke, S. D. Dods, D. Hewitt, and J. C. Li, "Multi impairment monitoring for optical networks," *J. Lightw. Technol.*, vol. 27, no. 16, pp. 3729–3736, Aug. 15, 2009.

[4] B. Kozicki, A. Maruta, and K.-i. Kitayama, "Experimental demonstration of optical performance monitoring for RZ-DPSK signals using delay-tap sampling method," *Opt. Exp.*, vol. 16, no. 6, pp. 3566–3576, Mar. 17, 2008.

[5] L. H. Cheng, Z. H. Li, C. Lu, A. P. T. Lau, H. Y. Tam, and P. K. A. Wai, "Chromatic dispersion monitoring based on variance of received optical power," *IEEE Photon. Technol. Lett.*, vol. 23, no. 8, pp. 486–488, Apr. 2011.

[6] J. Zhao, A. P. T. Lau, K. K. Qureshi, Z. H. Li, C. Lu, and H. Y. Tam, "Chromatic dispersion monitoring for DPSK systems using RF power spectrum," *J. Lightw. Technol.*, vol. 27, no. 24, pp. 5704–5709, Dec. 2009.

[7] Y. K. Lize, L. Christen, J. Y. Yang, P. Saghari, S. Nuccio, A. E. Willner, and R. Kashyap, "Independent and simultaneous monitoring of chromatic and polarization-mode dispersion in OOK and DPSK transmission," *IEEE Photon. Technol. Lett.*, vol. 19, no. 1, pp. 3–5, Jan. 1, 2007.

[8] J. Yang, C. Y. Yu, Y. F. Yang, L. H. Cheng, Z. H. Li, C. Lu, A. P. T. Lau, H. Y. Tam, and P. K. A. Wai, "PMD-insensitive CD monitoring based on RF clock power ratio measurement with optical notch filter," *IEEE Photon. Technol. Lett.*, vol. 23, no. 21, pp. 1576–1578, Nov. 1, 2011.

[9] T. D. Vo, B. Corcoran, J. Schroder, M. D. Pelusi, D.-X. Xu, A. Densmore, R. Ma, S. Janz, D. J. Moss, and B. J. Eggleton, "Silicon-chip-based real-time dispersion monitoring for 640 Gbit/s DPSK signals," *J. Lightw. Technol.*, vol. 29, no. 12, pp. 1790–1796, Jun. 15, 2011.

[10] J. Y. Yang, L. Zhang, X. Wu, O. F. Yilmaz, B. Zhang, and A. E. Willner, "All-optical chromatic dispersion monitoring for phase-modulated signals utilizing cross-phase modulation in a highly nonlinear fiber," *IEEE Photon. Technol. Lett.*, vol. 20, no. 19, pp. 1642–1644, Oct. 1, 2008.

[11] N. Liu, W. D. Zhong, Y. J. Wen, and Z. H. Li, "New transmitter configuration for subcarrier multiplexed DPSK systems and its applications to chromatic dispersion monitoring," *Opt. Exp.*, vol. 15, no. 3, pp. 839–844, Feb. 5, 2007.

[12] Z. H. Li, C. Lu, Y. X. Wang, and G. F. Li, "In-service signal quality monitoring and multi-impairment discrimination based on asynchronous amplitude histogram evaluation for NRZ-DPSK systems," *IEEE Photon. Technol. Lett.*, vol. 17, no. 9, pp. 1998–2000, Sep. 2005.

[13] Z. Li and G. Li, "Chromatic dispersion and polarization-mode dispersion monitoring for RZ-DPSK signals based on asynchronous amplitude-histogram evaluation," *J. Lightw. Technol.*, vol. 24, no. 7, pp. 2859–2866, Jul. 2006.

[14] Z. H. Li and G. F. Li, "In-line performance monitoring for RZ-DPSK signals using asynchronous amplitude histogram evaluation," *IEEE Photon. Technol. Lett.*, vol. 18, no. 3, pp. 472–474, Feb. 1, 2006.

[15] T. S. R. Shen, K. Meng, A. P. T. Lau, and Z. Y. Dong, "Optical performance monitoring using artificial neural network trained with asynchronous amplitude histograms," *IEEE Photon. Technol. Lett.*, vol. 22, no. 22, pp. 1665–1667, Nov. 2010.

[16] W. Carl, C. Schmidt, and H. G. Weber, "Application of asynchronous amplitude histograms for performance monitoring of RZ signals," in *Proc. OFC*, 2001, pp. WDD41-1–WDD41-3.

[17] I. Shake and H. Takara, "Averaged Q-factor method using amplitude histogram evaluation for transparent monitoring of optical signal-to-noise ratio degradation in optical transmission system," *J. Lightw. Technol.*, vol. 20, no. 8, pp. 1367–1373, Aug. 2002.

[18] Z. H. Li, C. Lu, Y. Dong, Y. X. Wang, T. H. Cheng, and F. M. Yue, "Asynchronous sampling for Q-factor estimation using sampling pulse with wide pulsewidth," *IEEE Photon. Technol. Lett.*, vol. 15, no. 12, pp. 1749–1751, Dec. 2003.

[19] R. Luis, P. Andre, A. Teixeira, and P. Monteiro, "Performance monitoring in optical networks using asynchronously acquired samples with nonideal sampling systems and intersymbol interference," *J. Lightw. Technol.*, vol. 22, no. 11, pp. 2452–2459, Nov. 2004.

[20] P. J. Winzer and R. J. Essiambre, "Advanced optical modulation formats," *Proc. IEEE*, vol. 94, no. 5, pp. 952–985, May 2006.

[21] G. P. Agrawal, *Nonlinear Fiber Optics,* 3rd ed. New York: Academic, 2001.